

## **RESEARCH ON PREPARATION AND PROPERTIES OF C-S-H /PEG1000 PHASE CHANGE COMPOSITE**

**Chen Chen (1), Qi Zheng (1) and Jinyang Jiang \*(1)**

(1) School of Materials Science and Engineering, Southeast University, China

### **Abstract**

In this paper, composite material C-S-H/PEG1000 was prepared by multi-scale porous material C-S-H as support and phase change material (PCM) PEG1000 by melt blending, so that it can reduce hydration heat of cementitious system utilizing the characteristics of releasing and storing energy of PCM. TEM, IR, DSC-Tg, BET, MIP and various other characterization methods were used to discuss the feasibility of C-S-H as carrier and investigate the morphology, pore structure and stability of the C-S-H/PEG1000 composite. The change of hydration heat and features of pore structure as well as its effect on compressive strength were also tested when the composite was added into the cementitious system. Study shows that the PEG1000 can be well embedded into the hollow inside space of C-S-H to form dense blocks in the form of physical adsorption, with good bonding state and thermal stability, which can decrease heat releasing rate and total heat of the hydration process in cementitious system. The early strength was pretty influenced with different addition of C-S-H/PEG1000, however, the later strength was improved.

Keywords: calcium silicate hydrate; phase change material composite; pore structure; hydration heat; thermal stability

### **1. INTRODUCTION**

In recent years, PCMs has been widely applied in various fields owing to their high latent heat storage density, small volume changes and fixed phase change temperature range <sup>[1]</sup>. For constructions, this feature has great potential in terms of saving energy <sup>[2]</sup>, such as concrete walls and insulating layers. Generally speaking, the integration of PCMs and supports into architectural fabrics can effectively exert this characteristic <sup>[3,4]</sup>. Similarly, suitable phase change materials can also be used to solve the problem of thermal stress caused by the massive release of hydration heat in short term.

Due to the large thermal stress caused by internal temperature difference, mass concrete and other projects demand extremely low thermal cement based materials. The ABAQUS simulation illustrated in the Fig.1 demonstrates the concrete adiabatic temperature rise and thermal stress distribution, in which the highest initial internal temperature is up to 70°C and nearly 40 hours are costed to cool down completely, similar to existed works <sup>[5]</sup>. It shows that it is in urgent need of phase change energy storage material with a certain temperature, so the proposed research of C-S-H/PEG1000 is of importance and necessity in building materials field.

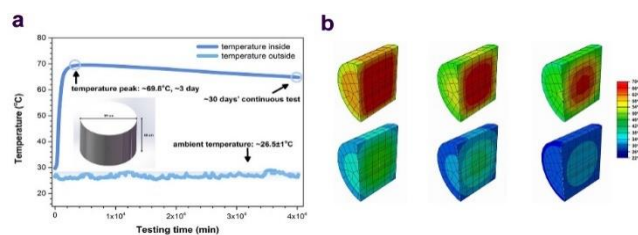


**Figure 1: ABAQUS simulation of adiabatic temperature rise (a) and thermal stress distribution (b).**

PEG1000 is PCM with a large latent heat capacity, 152.9 J/g measured in this work. Combining PEG with other porous materials, such as porous silica [6], MCS [8] and LA [12], is an effective way to use thermal properties to produce new smart materials and avoid leakage. Zhang et al. [10] studied the phase change properties of PEG blends with PP, PET or ethylene vinyl acetate, while the materials tend to lose their phase change characteristics after several heating cooling cycles due to the loss of PEG. Hu et al. [9] prepared a solid-solid PCM by poly-PEG. However, even the maximum enthalpy was still low. Therefore, in order to apply it stably and efficiently in cement, it is necessary to ensure the combination stability and chemical stability with appropriate support.

CSH is a kind of material with multi-scale pore structure. The pores of CSH can be divided into three parts [14]: the pores caused by the accumulation of large particles (> 200nm), medium particles (50-200 nm) and small particles (< 50nm), the intrinsic pores inside the particles, and the interlayer pores at the level of C-S-H structure. C-S-H is a common and readily available hydration product of porous cement.

In this work, a phase change composite material C-S-H/PEG1000, which can effectively reduce the heat of hydration, was prepared by combining cement basic hydration product C-S-H with PEG1000 innovatively. The feasibility and rationality of the support were deduced through simulation model and experimental characterization, and the properties of the phase change composite were characterized, including morphology, pore structure, stability, etc., which were mutually verified with the experimental results of hydration heat and compressive strength on the macro level. To sum up, we provided some new insights to C-S-H design and application of energy absorption and storage performance of PCMs for cement-based materials.

## 2. EXPERIMENTAL

### 2.1 Materials

Tricalcium silicate (C<sub>3</sub>S), Polyethylene glycol (PEG1000), were purchased from Sinopharm Chemical Reagent Co., Ltd. All these chemicals were used as received without further purification. Deionized water ( $\Omega > 18\text{M}\Omega \text{ cm}$ , 25°C) and ethanol (99.7%) were used throughout.

### 2.2 Methods

#### 2.2.1 Preparation of C-S-H

C-S-H was prepared by hydration of C<sub>3</sub>S at room temperature. C<sub>3</sub>S powder was dissolved in deionized water with the mass ratio of water to solid by 125:1 in the beaker. After suspension for 72h with continuous stirring on magnetic mixer, the precipitates were collected and separated by vacuum filtration over a 0.45 $\mu\text{m}$  membrane. The filter cake was re-dispersed and filtered and repeated for times to remove salts and unwanted ions like the by-product Ca(OH)<sub>2</sub>. The final filter cake was dried at 150°C, and C-S-H was obtained by grinding and sieving.

## 2.2.2 Preparation of C-S-H/PEG1000

After the synthesis of C-S-H, thermal-stabilized phase change materials composite was prepared by a facile blending and impregnating method. PEG were intercalated into C-S-H porous structure in specific procedures. Firstly, C-S-H and PEG1000 were proportionally mixed in a mass ratio of 1:1.6, and then the mixture was processed at 70°C for 2h with stirring. Ultimately, the C-S-H/PEG1000 was cooled, grinding and sieving for further characterization.

## 2.2.3 Analysis methods

The particle size distribution was measured by laser diffraction particle size analyzer. The morphology was investigated by SEM and TEM. XRD patterns were collected at a scanning rate of 0.15 s/step with 0.02° step size in the 2θ range 5~60° using Ni-filtered CuKα radiation and operating at 40 kV and 30 mA. The BET surface areas and BJH pore-size distributions were measured with analyzer. MIP was also adopted to calculate the pore volume and pore-size distributions. Different phase distribution was investigated by a high resolution 3D X-ray microscope. The FT-IR spectra were recorded in the wavenumber region between 400 cm<sup>-1</sup> and 4000 cm<sup>-1</sup>. The phase change temperature and enthalpy were obtained by using DSC-TG. Zeta potential was investigated to explain the stability of C-S-H/PEG1000.

## 3. RESULTS AND DISCUSSION

### 3.1 Simulation of C-S-H

The model construction of C-S-H was based on the procedures proposed by Pellenq, Manzano and Qomi [7,13]. The calcium to silicon ratio was controlled at 1.5 according to experimental results. The multi-scale pore structure of C-S-H was obtained by building a C-S-H model between particles and atoms at different scales, as shown in Fig. 2, which provided theoretical basis for its rationality as a carrier.

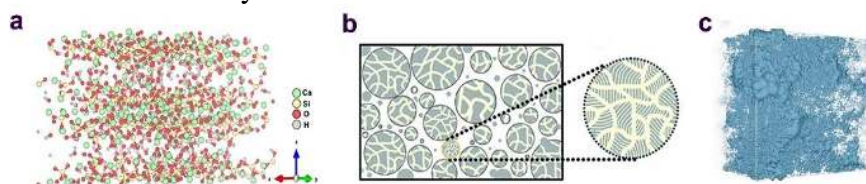


**Figure 2: Construction multi-scale pore structure models of C-S-H including the micro model (a), mesoscopic model (b) and macro model (c).**

### 3.2 Characterization of C-S-H/PEG1000

Particle size analysis was carried out and the average size of monodispersity C-S-H is 21.89μm approximating to a normal distribution shown in Fig. 3. For composite, part of PEG1000 enters and fills the internal pores and part is wrapped on the surface. As a result, the particle size of the composite material after grinding becomes thicker and larger, and shows a bimodal distribution with the average size of 45.01μm. The value of two peaks appears at approximately 13μm and 115μm, related to the uniformity of the wrapping.

SEM and TEM images exhibited in Fig. 4 show the morphology of C-S-H and C-S-H/PEG1000. Fig. 4(a, b) shows the cluster morphology of C-S-H composed of sheets of nanometers. Randomly oriented hydration products are staggered and stacked, showing stratified pores between clusters, forming a 3D network structure. Moreover, a typical high resolution TEM image in Fig. 4 (e) shows C-S-H is amorphous thin-layer structure similar to

'silica gardens' structure of Double. These nanosheets are likely to fold, crinkling and stacking, corresponding to the results of SEM.

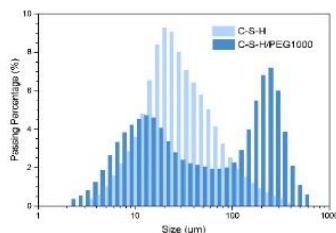


**Figure 3: Particle size distribution of synthetic C-S-H and C-S-H/PEG1000.**

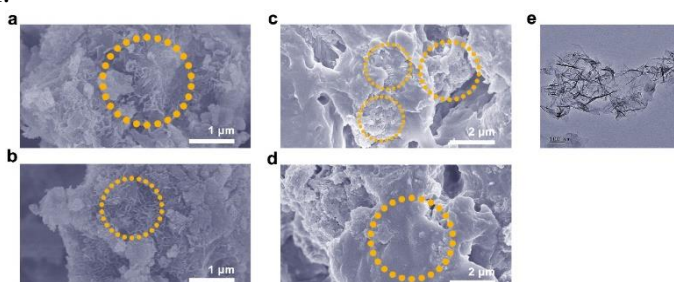


**Figure 4: Micrographs of C-S-H (a, b) and C-S-H/PEG1000 (c, d) obtained by SEM (a-d) and C-S-H by TEM (e). Scale bars are 1μm, 2μm and 100 nm, respectively.**

Subsequently, it could be found in Fig. 4(c, d) that PEG1000 change the morphology of C-S-H when cooperated into it. The morphology presented in the yellow circle can be seen that PEG1000 molecules embedded in the hollow space of C-S-H perfectly. Namely, PEG1000 is loaded on the multi-scale pore structure of C-S-H to form a compact and dense C-S-H/PEG1000 block by blocking and filling the pores. Due to the coating effect of PEG1000 on the surface of C-S-H, the surface of composite becomes more smooth than C-S-H. Most importantly, no leakage of PEG1000 is observed in Fig. 4(c, d), confirming the stability of C-S-H/PEG1000 composites. Even after dozens of thermal-cold cycling treatment, there was little leakage of PEG1000 can be seen, suggesting that the PEG1000 is well impregnated into C-S-H pores and C-S-H/PEG1000 is successfully synthesized as a composite.

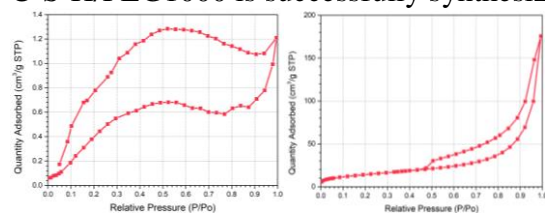


**Figure 5: N<sub>2</sub>-adsorption-desorption isotherms of C-S-H (a) and C-S-H/PEG1000 (b).**

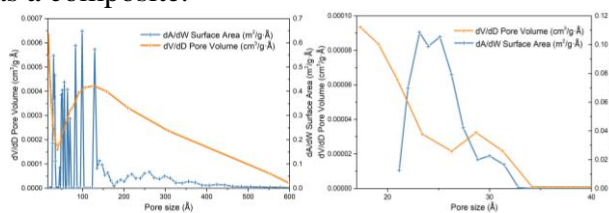


**Figure 6: BJH-desorption pore-size-distribution curves of C-S-H (a) and C-S-H/PEG1000 (b)**

The porous characteristics of the C-S-H and C-S-H/PEG1000 is examined by BET. As Fig.5 presents, the N<sub>2</sub> adsorption-desorption isotherm of C-S-H matches the type III isotherm in the Brunauer classification corresponding to a solid material with large pores. And it exhibits type H3 hysteresis loop according to IUPAC, which is commonly found in layered aggregates, forming mesoporous or macroporous materials in the shape of slits. Demonstrated characteristic features is in good accordance with SEM and TEM observations. The pore size distribution of C-S-H is reflected by BJH model. As is shown in Fig.6 (a), the results suggest abundant specific surface area about 52.5 m<sup>2</sup>/g measured by BET and a wide range of pore size distribution ranging from 17 to 600Å of C-S-H, the most probable pore size of which is at 125.17Å. This multi-scale pore structure enables C-S-H to carry amount of PCM of different particle sizes.

The multi-scale pores of C-S-H can be divided into three parts: pores caused by the accumulation of large particles (>200nm), medium particles (50-200nm) and small particles (<50nm), intrinsic pores inside the particles, and interlayer pores on the C-S-H structure level.

Fig. 5 (b) and Fig.6 (b) provide that the specific surface area of C-S-H/PEG1000 decreases more than 90% which is  $3.3075\text{m}^2/\text{g}$  measured by BET method, and the mean pore size of BJH-desorption is  $25.787\text{\AA}$  dropping around 80%. Moreover, BJH Desorption cumulative volume of pores between  $17\text{\AA}$  and  $3,000\text{\AA}$  diameter of C-S-H and C-S-H/PEG1000 are  $0.27\text{ cm}^3/\text{g}$  and  $0.0020\text{ cm}^3/\text{g}$ , respectively. When PEG is introduced into C-S-H, the pores of C-S-H larger than 4 nm are almost completely contained by PEG1000 molecules, resulting in a high proportion of pores at the center of 2 nm. The steep decrease in specific surface area, pore volume, and pore size combined with the electron microscopy results proves that the PEG1000 could indeed fill the multi-scale pores of C-S-H. combination with the support can change the texture and morphology of the PCM, providing convenience for the incorporation of PCM, so that many problems of incorporation of single PCM are avoided. Therefore, it is necessary to introduce PCM support into the cement based composite material.

As mentioned above, porous characteristics and multi-scale pore structure of c-s-h were clearly illustrated by means of electron microscopy imaging and pore structure analysis. The structure feasibility of composite using C-S-H as a support is proved, which provides a premise for the perfect filling and stable composite to achieve the aim of efficient energy storage. In addition, as one of the main hydration products of cement, the incorporation of c-s-h can avoid unknown adverse reactions, and at the same time, C-S-H can prevent the leakage of phase change materials during energy absorption and energy release, so that the composite material has excellent working performance and high energy absorption efficiency.

### 3.3 Stability of C-S-H/PEG1000

The weak characteristic peak of C-S-H (I) around  $30^\circ$  in XRD patterns in Fig.7 shows that the sample is amorphous gel of low crystallinity degree. The main characteristic peaks ( $d=0.303\text{nm}$ ,  $0.277\text{nm}$  and  $0.192\text{nm}$ ) are basically consistent with the literature<sup>[11]</sup>. Furthermore,  $\text{Ca}(\text{OH})_2$  characteristic peak ( $d=0.488\text{nm}$ ,  $0.261\text{nm}$ ,  $0.192\text{nm}$ ) can be seen around  $18^\circ$ , which is the residual hydration products after washing. The XRD of C-S-H/PEG1000 is superposition of C-S-H and PEG1000. No obvious characteristic peak of new phase is found, meaning it is probably a simple physical combination between them. The chemical compatibility of composite is shown in Fig. 8. From bottom th top, spectra nanometers stretching vibration at  $1480$  and  $960\text{ cm}^{-1}$ . The peak at  $1355\text{ cm}^{-1}$  is caused by C-O-C, while peaks of C-O is also found at  $1650\text{ cm}^{-1}$  and  $1110\text{ cm}^{-1}$ . In addition, the

characteristic peaks for stretching vibration of -OH at  $3450\text{ cm}^{-1}$ .

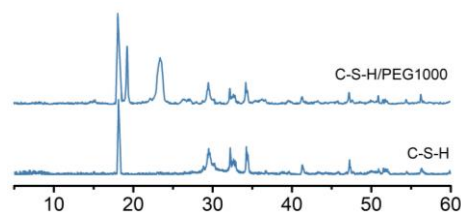


Figure 7: XRD of C-S-H and C-S-H/PEG1000

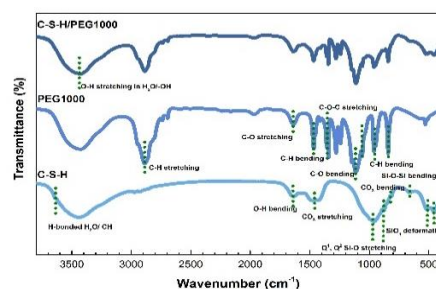
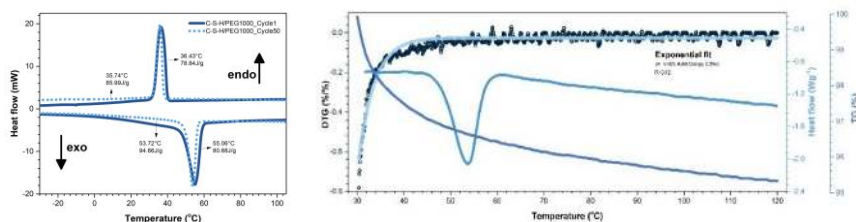


Figure 8: IR of C-S-H/PEG1000

From the perspective of C-S-H, the peaks of O-H, Si-O-Si and  $\text{SiO}_4$  tetrahedrons are found Peaks at  $870$  and  $970\text{ cm}^{-1}$  could be ascribed to the stretching vibration of Si-O groups in  $\text{Q}^1$  or  $\text{Q}^2$  states. Compared with PEG1000 and C-S-H, no obvious new peaks generating in the spectra

of composite. The physical binding between them is controlled by weak Vanderwals force without other obvious chemical interactions. Based on the vulnerable physical sorption, the PEG1000 molecules can accommodate in C-S-H pore structures recyclable and sustainable. It reveals the chemical compatibility between the C-S-H and PEG1000 conforming to the XRD.



**Figure 9: DSC-TG curves of C-S-H/PEG1000 after thermal-cold cycles**

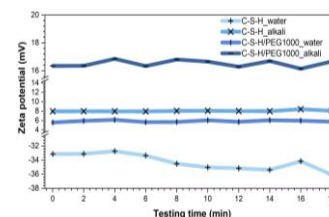


**Figure10: Zeta potential of C-S-H and composite.**

DSC and TG are conducted to investigate long-term thermal stability in variable temperature environment to ensure the its effective service. The phase change temperature ranges from 30 to 60°C in Fig. 9, equivalent to hydration heat. The loss of weight and phase change enthalpy are within reasonable value, and DTG curve follows the equation  $y = -0.025 - 4386.55 \exp(-0.29x)$ . Until temperature raised to 120 °C, the mass loss rate of composite is less than 5%, showing good thermal stability. The thermal stability properties were performed by 50 thermal-cold cycles. The peak temperature of endothermic and exothermic are 35.74 and 53.72°C now, while the latent heat are 85.99 and 80.68 J/g, closed to data of first cycle. It is remarkably noted that the form-stable C-S-H/PEG1000 shows good thermal reliability and bonding stability regarding to its slight change in phase change temperatures and latent heat. These strong evidence suggest that composite is chemically, thermally and structurally stable during working.

As a complement, the Zeta potential are relatively stable in alkali and aqueous solution with the extension of testing time. There are no significant fluctuations, therefore the combination stability and chemical stability of the support C-S-H and the new prepared composite are verified. C-S-H/PEG1000 composite can work in cement based materials steadily and well.

Various characterization of the performance of C-S-H/PEG1000 indicate that PEG1000 can be well loaded on c-s-h, and it has good adaptability and stability in cement system.

### 3.4 Performance analysis of C-S-H/PEG1000 in cement system

#### 3.4.1 Hydration heat

Phase change composite is added into the PII 525 cement replacing 0% to 20% binding material (W/C=0.5). Fig. 11 shows the change of hydration heat of cement system with the increase of C-S-H/PEG1000 to explore the effect of energy absorption and storage. With the content of composite raised up to 20%, the peak height of rate decrease significantly, meanwhile the peaks move right and become wider obviously, indicating that hydration rate slows down. Total amount of hydration heat decreases, which is reduced to half under the condition of 20%, indicating that C-S-H/PEG1000 could play a good role in energy absorption and energy storage. The existence of PCM reduces the hydration heat and slowed down the hydration process.

#### 3.4.2 Compressive stress

The compressive strength of blocks with different dosage of the C-S-H/PEG1000 curing for 3d to 28d is shown in the Fig.12, as well as the contrast added in pure PEG. With the increase

of C-S-H/PEG1000, the compressive strength shows a downward trend at all age. The influence on early strength is relatively great, however, the later strength rises distinctly. And the later strength after 14d is almost not affected at low dosage of the composite. Compared with blocks with PEG1000 alone, strength decreases to the half. The results indicate that the combination with C-S-H and PEG1000 improves the compressive strength when used in cement system at the same dosage and curing age. Hence, taking advantage of C-S-H as support is necessary.

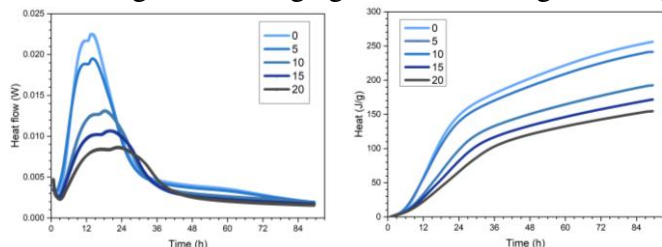


**Figure 11: Hydration heat of cement incorporated with C-S-H /PEG1000.**

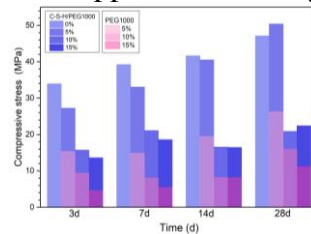


**Figure 12: Compressive stress of different cement blocks.**

### 3.4.3 Microstructure

SEM images in Fig.13 show the morphology of blank samples and blocks incorporated in 15% composite. The former is denser with a large number of needle-like hydration products overlapping. C-S-H has lost its cementitious property in composite due to complete hydration. In contrast, the cementitious products in the pores and micro-cracks are reduced (orange circles) and the texture was more loose (green circles) for C-S-H/PEG1000 replaced cement blocks.

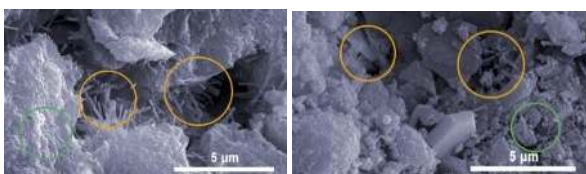


**Figure 13: SEM of blocks incorporated with 0% and 15% C-S-H/PEG1000**

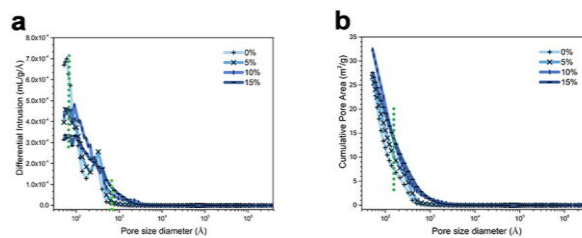


**Figure 14: Pore size distribution and pore area of blocks with different amount of C-S-H/PEG1000 curing for 28d**

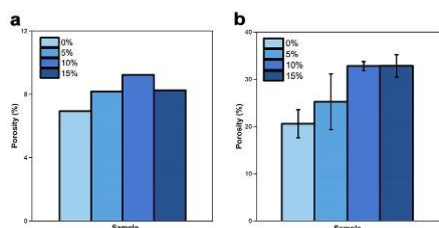
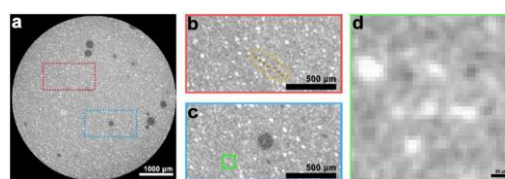


**Figure 15: Porosity of cement blocks obtained by MIP (a) and 3D computed tomography segregation (b) curing for 28d**



(a) Original X-CT image of blank cement blocks. The black areas represent the pores. The scale is 1000μm. - (b) The red box area is enlarged in Fig. 16 (b) and the internal cracks are highlighted in brown dotted line. - (c) The blue box area is enlarged in Fig. 16 (c) and the unhydrated cement particles are highlighted in green dotted box. (d) Grayscale image in pixels with a scale of 20μm. The size of each pixel is 5.0μm. -

**Figure 16: Schematic diagram of computed tomography obtained by 3D microscope**

MIP results reflect the pore structure of the cement blocks and the gray value obtained from high resolution 3D X-ray microscope can be used to analyze the distribution of different phases, including pores, cracks and unhydrated cement particles in Fig.16. Accordingly, the internal microstructure is explored. in Fig. 14 and Fig. 15, the blocks gain more pore volume and area

when composite gradually increases from the results calculated by MIP and CT. Consistent with the regular of SEM, the porosity increases and the compactness is affected with the improvement of composite, reflecting the damage of compressive strength at the macro level.

#### 4. CONCLUSIONS

- A preparation method of C-S-H/PEG1000 phase change composite was introduced.
- The multi-scale and rich pore structure of C-S-H is analysed through simulation and experiments, and its feasibility and rationality as a support for PCM are demonstrated.
- C-S-H/PEG1000 phase change composite material has not only the suitable phase change temperature range and large latent heat, but also the good chemical and thermal stability.
- Composite can effectively slow down the hydration rate and reduce the total heat in cement system. Moreover, direct incorporation of PEG1000 will greatly damage the compressive strength compared with C-S-H/PEG1000, for which the early strength is influenced to a certain extent while and the later strength will gradually increase.

#### REFERENCES

- [1] Pellenq J M, Kushima A, Shahsavari R, et al. A realistic molecular model of cement hydrates[J]. Proceedings of the National Academy of Sciences, 2009, 106(38):16102-16107.
- [2] Memon SA. Phase change materials integrated in building walls: a state of the art review. Renew Sustain Energy Rev 2014; 31:870-906.
- [3] Frédéric Kuznik, David D, Johannes K, et al. A review on phase change materials integrated in building walls[J]. Renewable and Sustainable Energy Reviews, 2011, 15(1):379-391.
- [4] Ramakrish S, et al. Thermal performance of buildings integrated with phase change materials to reduce heat stress risks during extreme heatwave events[J]. Applied Energy, 2016, 194:410-421.
- [5] Han F, et al. Study on mix proportion optimization and performance of mass concrete [J]. Concrete world, 2014(3):66-69.
- [6] Wang J, Yang M, Lu Y, et al. Surface functionalization engineering driven crystallization behavior of polyethylene glycol confined in mesoporous silica for shape-stabilized phase change materials[J]. Nano Energy, 2015, 19:78-87.
- [7] Pellenq RJ-M, Kushima A, Shahsavari R, Van Vliet KJ, Buehler MJ, Yip S, et al. A realistic molecular model of cement hydrates. Proc Natl Acad Sci 2009; 106:16102-7.
- [8] Qian T, Li J, Min X, et al. Polyethylene glycol/mesoporous calcium silicate shape-stabilized composite phase change material: Preparation, characterization, and adjustable thermal property[J]. Energy, 2015, 82:333-340.
- [9] Hu J, Yu H, Chen Y, et al. Study on Phase Change Characteristics of PET - PEG Copolymers[J]. Journal of Macromolecular Science, Part B, 2006, 45(4):615-621.
- [10] Liang X H, Guo Y Q, Gu L Z, et al. Crystalline-Amorphous Phase Transition of Poly (ethylene Glycol)/Cellulose Blend[J]. Macromolecules, 1995, 28(19):6551-6555.
- [11] Zhao X. Synthesis of calcium silicate hydrate and its composition, structure and morphology [D]. Wuhan university of technology, 2010.
- [12] Jiang J, Zheng Q, Yan Y, et al. Design of a novel nanocomposite with C-S-H@LA for thermal energy storage: A theoretical and experimental study[J]. Applied Energy, 2018, 220:395-407.
- [13] Manzano H, et al. Confined water dissociation in microporous defective silicates: mechanism, dipole distribution, and impact on substrate properties. J Am Chem Soc 2012; 134:2208-15.
- [14] Wenzel O, Schwotzer M, Müller E, Chakravadhanula VSK, Scherer T, Gerdes A. Investigating the pore structure of the calcium silicate hydrate phase. Mater Charact 2017; 133:133-7.